First observation of the production of nucleon resonances in $\bar{\mathrm{p}}$ annihilation in deuterium

Crystal Barrel Collaboration

C. Amsler[o], D.S. Armstrong[a 1], I. Augustin[h 2], C.A. Baker[e], B.M. Barnett[c], C.J. Batty[e], M. Benayoun[f], K. Beuchert[b], P. Birien[a], P. Blüm[h], R. Bossingham[a], K. Braune[m], J. Brose[k], D.V. Bugg[i], M. Burchell[f 3], T. Case[a], A. Cooper[i], O. Cramer[m], K.M. Crowe[a], T. Degener[b], H.P. Dietz[m], N. Djaoshvili[f], S. v. Dombrowski[o], M. Doser[f], W. Dünnweber[m], D. Engelhardt[h], M. Englert[m], M.A. Faessler[m], C. Felix[m], G. Gemesy[d], P. Giarritta[o], R. Hackmann[c], R.P. Haddock[j], F.H. Heinsius[a], M. Herz[c], N.P. Hessey[f], P. Hidas[d], P. Illinger[m], D. Jamnik[m4], H. Kalinowsky[k], B. Kalteyer[c], B. Kämmle[g], T. Kiel[h], J. Kisiel[f 5], E. Klempt[c], M. Kobel[f 6], H. Koch[b], C. Kolo[m], K. Königsmann[m7], M. Kunze[b], M. Lakata[a], R. Landua[f], J. Lüdemann[b], H. Matthaey[b], R. McCrady[l], M. Merkel[k 8], J.P. Merlo[k], C.A. Meyer[l], L. Montanet[f], A. Noble[o 9], R. Ouared[f], F. Ould–Saada[o] K. Peters[b], C.N. Pinder[e], S. Ravndal[b 10], C. Regenfus[m], S. Resag[c], E. Schäfer[k], P. Schmidt[g], R. Seibert[g], S. Spanier[o], H. Stöck[b], C. Straßburger[c], U. Strohbusch[g], M. Suffert[n], U. Thoma[c 11], M. Tischhäuser[h], D. Urner[o], C. Völcker[m], F. Walter[k], D. Walther[b], U. Wiedner[g], N. Winter[h], J. Zoll[f], B.S. Zou[i], Č. Zupančič[m]

[a] *University of California, LBL, Berkeley, CA 94720, USA*
[b] *Universität Bochum, D-44780 Bochum, FRG*
[c] *Universität Bonn, D-53115 Bonn, FRG*
[d] *Academy of Science, H-1525 Budapest, Hungary*
[e] *Rutherford Appleton Laboratory, Chilton, Didcot OX11 0QX, UK*
[f] *CERN, CH-1211 Genève, Switzerland*
[g] *Universität Hamburg, D-22761 Hamburg, FRG*
[h] *Universität Karlsruhe, D-76021 Karlsruhe, FRG*
[i] *Queen Mary and Westfield College, London E1 4NS, UK*
[j] *University of California, Los Angeles, CA 90024, USA*
[k] *Universität Mainz, D-55099 Mainz, FRG*
[l] *Carnegie Mellon University, Pittsburgh, PA 15213, USA*
[m] *Universität München, D-80333 München, FRG*
[n] *Centre de Recherches Nucléaires, F-67037 Strasbourg, France*
[o] *Universität Zürich, CH-8057 Zürich, Switzerland*

Received ; revised manuscript received

We report the observation of nucleon resonances in the reaction $\bar{\mathrm{p}}\mathrm{d} \to \pi^0\pi^0\mathrm{n}$ for antiprotons stopping in liquid deuterium. The process $\bar{\mathrm{p}}\mathrm{d} \to \Delta(1232)\pi^0$ is identified and its rate determined to be $(2.21 \pm 0.24)\cdot 10^{-5}$.

[1]Now at William & Mary College, Williamsburg, VA 23187, USA

[2]Now at Universität Siegen, Siegen, Germany

[3]Now at University of Kent, Canterbury, UK

[4]On leave of absence from the University of Ljubljana,

It is well known that antiproton annihilation in deuterium occurs preferently on quasi-free nucleons leaving one nucleon as "spectator" with a typical momentum of 100 MeV/c [1]. However, in a large fraction of events the nucleon observed in the final state has a wide momentum distribution ranging from low momenta up to the kinematical limit (see, e.g., figure 3c below). The occurence of non-spectator events is usually explained as a two step process. Antiprotons annihilate on one nucleon producing a number of pions; one of the pions scatters off the second nucleon forming a nucleon resonance. Their decay products then have a wide momentum distribution.
In any case, even if the above mechanism is put in doubt, antiproton annihilation in deuterium allows production of nucleon resonances. We represent the initial $\bar{\mathrm{p}}$d atomic state in the spectroscopic notation $^{(2I+1)(2S+1)}L_J$, nucleon resonances by their partial wave $L_{2I,2J}$. Annihilation in deuterium may occur from S or P angular momentum states (L); the isospin of the initial state is necessarily I=1/2. In S-states, the $\bar{\mathrm{p}}$d system may have a total spin ($J = S$) of 1/2 or 3/2. In case of P-states, J can be 1/2, 3/2, 5/2. Table 1 summarizes the possible quantum numbers in N* or Δ production.

initial state	nucleon resonance	ℓ (production)
$^{22}S_{1/2}$	P_{11}, P_{31}	0
	S_{11}, S_{31}, D_{13}, D_{33}	1
	P_{13}, P_{33}	2
$^{24}S_{3/2}$	P_{13}, P_{33}	0
	S_{11}, S_{31}, D_{13}, D_{33}	1
	P_{11}, P_{31}, P_{13}, P_{33}	2
$^{22}P_{1/2}$, $^{24}P_{1/2}$	S_{11}, S_{31}	0
	P_{11}, P_{31},P_{13}, P_{33}	1
	D_{13}, D_{33}	2
$^{22}P_{3/2}$, $^{24}P_{3/2}$	D_{13}, D_{33}	0
	P_{11}, P_{31}, P_{13}, P_{33}	1
	S_{11}, S_{31}, D_{13}, D_{33}	2
$^{24}P_{5/2}$	P_{13}, P_{33},	1
	S_{11}, S_{31}, D_{13}, D_{33}	2

Table 1
Quantum numbers of the initial states of antiproton annihilation in deuterium and possible quantum numbers of nucleon resonances which may be produced with low relative orbital angular momentum ($\ell \leq$2).

In this letter we report on the first observation of the reaction

$$\bar{\mathrm{p}}\mathrm{d} \rightarrow \pi^0\Delta^0\,;\;\; \Delta^0 \rightarrow \pi^0\mathrm{n} \quad (1)$$

and determine its production rate. Evidence for production of higher–mass states is also reported.
In addition we extract the branching ratio for

$$\bar{\mathrm{p}}\mathrm{d} \rightarrow \pi^0\pi^0\mathrm{n} \quad (2)$$

and $\bar{\mathrm{p}}\mathrm{d} \rightarrow \pi^0\eta\mathrm{n}$. (3)

The data were taken with the Crystal Barrel detector at the CERN Low Energy Antiproton Ring (LEAR) by stopping 200 MeV/c antiprotons in a liquid deuterium target. Details on the detector are given in [2]; here we recall only that charged particles are tracked in two cylindrical proportional wire chambers and a jet drift chamber with 23 layers, and that photons are detected in a modular CsI calorimeter with nearly 4π solid angle coverage. The analysis presented here is based on $4.23\cdot10^6$ $\bar{\mathrm{p}}$d annihilations recorded in two run periods with a "zero–prong" trigger selecting events with no observed charged particles in the final state. For normalisation $1.86\cdot10^6$ events were also taken with a "minimum bias" trigger requiring an antiproton entering the target but with no constraints on the final state. The data were submitted to a series of cuts rejecting events with residual tracks from charged particles, events in which a crystal surrounding the beam entrance or beam exit holes has a local energy maximum (to avoid energy loss along the beam pipe), and events not having exactly four showers in the CsI calorimeter.

The requirement of exactly four showers in the electromagnetic calorimeter restricts the events to those in which the neutron did not interact in the detector. The interaction probability for a neutron - leading to one additional shower in the

Ljubljana, Slovenia
[5] On leave of absence from the University of Silesia, Katowice, Poland
[6] Now at Universität Freiburg, Freiburg, Germany
[7] Now at Max Planck Institute, Heidelberg, Germany
[8] Now at CERN, Genève, Switzerland
[9] Now at CRPP, Ottawa, Canada
[10] Now at CERN, Genève, Switzerland
[11] This work is part of the thesis of U. Thoma

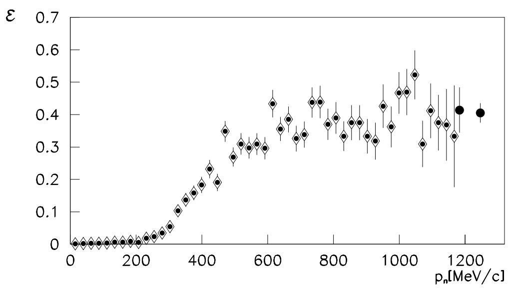

Fig. 1. *Momentum dependence of the neutron detection efficiency*

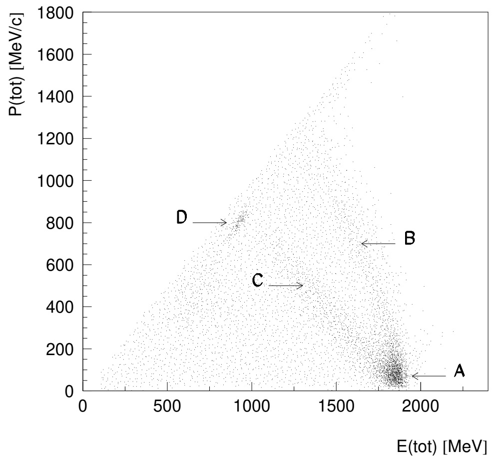

Fig. 2. *Total momentum versus total energy*

calorimeter- depends on its momentum; the neutron detection efficiency has been determined in [3] and is shown in figure 1.

The data are corrected for this probability of not observing the neutron. The acceptance of the two π^0 is nearly flat over the phase space. Possible background sources were studied by Monte Carlo simulations; their contributions were found to be negligible ($\leq 1\%$ and concentrated at neutron momenta $\leq$ 350 MeV/c)

Figure 2 shows a scatterplot of the total momentum versus total energy for the $4\gamma\, \mathrm{n}_{miss}$-final state.

The dominant contribution, at the lower right part (A), comes from the "quasi-free" $\bar{\mathrm{p}}\mathrm{p}$ annihilation into two π^0 leaving a spectator neutron at low momentum. The intensity band with the larger total mass originates from non-spectator events with missing neutron (B), the second band from events with one missing π^0 and a spectator neutron (C). The events with total energy of ~1000 MeV and total momentum of 800 MeV/c correspond to the reaction $\bar{\mathrm{p}}\mathrm{d}\rightarrow K^0_S K^0_L \mathrm{n}$ with $K^0_S\rightarrow\pi^0\pi^0$, an unseen K^0_L and a spectator neutron (D). After a cut on missing mass at $m_{miss} = m_{\mathrm{n}}\pm 150$ MeV and a 3-constraint kinematic fit on $\bar{\mathrm{p}}\mathrm{d}\rightarrow\pi^0\pi^0\mathrm{n}$ imposing π^0 masses we find 52432 events in the zero–prong data and 447 events in the minimum bias data. Similarly, we obtain 7539 events of the type $\bar{\mathrm{p}}\mathrm{d}\rightarrow\pi^0\eta\mathrm{n}$.

The $\pi^0\pi^0$n-Dalitz plot, which contains each event twice, is dominated by events with a spectator neutron. The more interesting contributions are revealed after a cut on the spectator momentum, $|\, \boldsymbol{p}_n \,| \geq 600$ MeV/c. This part of the Dalitz plot is shown in figure 3a after correcting for the probability that the neutron is undetected. The full Dalitz plot is shown as an inset of figure 3c.

The Dalitz plot is characterised by a vertical band at a $\pi^0\pi^0$ invariant mass of 1270 MeV which we assign to the reaction $\bar{\mathrm{p}}\mathrm{d}\rightarrow f_2(1270)$+n with $f_2(1270)\rightarrow\pi^0\pi^0$. Furthermore, there are three horizontal bands indicating the presence of N^* or Δ resonances. Due to the combinatorial ambiguity these bands occur as well in the diagonal direction. The positions of the resonances are indicated by arrows.

In a first attempt to identify the baryon resonances we apply a cut on the invariant $(\pi^0\pi^0)$ invariant mass, $m_{\pi^0\pi^0} \leq$1000 MeV, and plot the $(\pi^0\mathrm{n})$ invariant mass of the remaining events, see figure 3b. The lowest mass peak is readily assigned to the $\Delta(1232)$. The peak at 1650 MeV may contain contributions from N(1650) and/or $\Delta(1620)$; in the high-mass region several resonances are known to exist which may contribute to the observed peaks. With the present statistics, a full partial wave analysis in order to determine

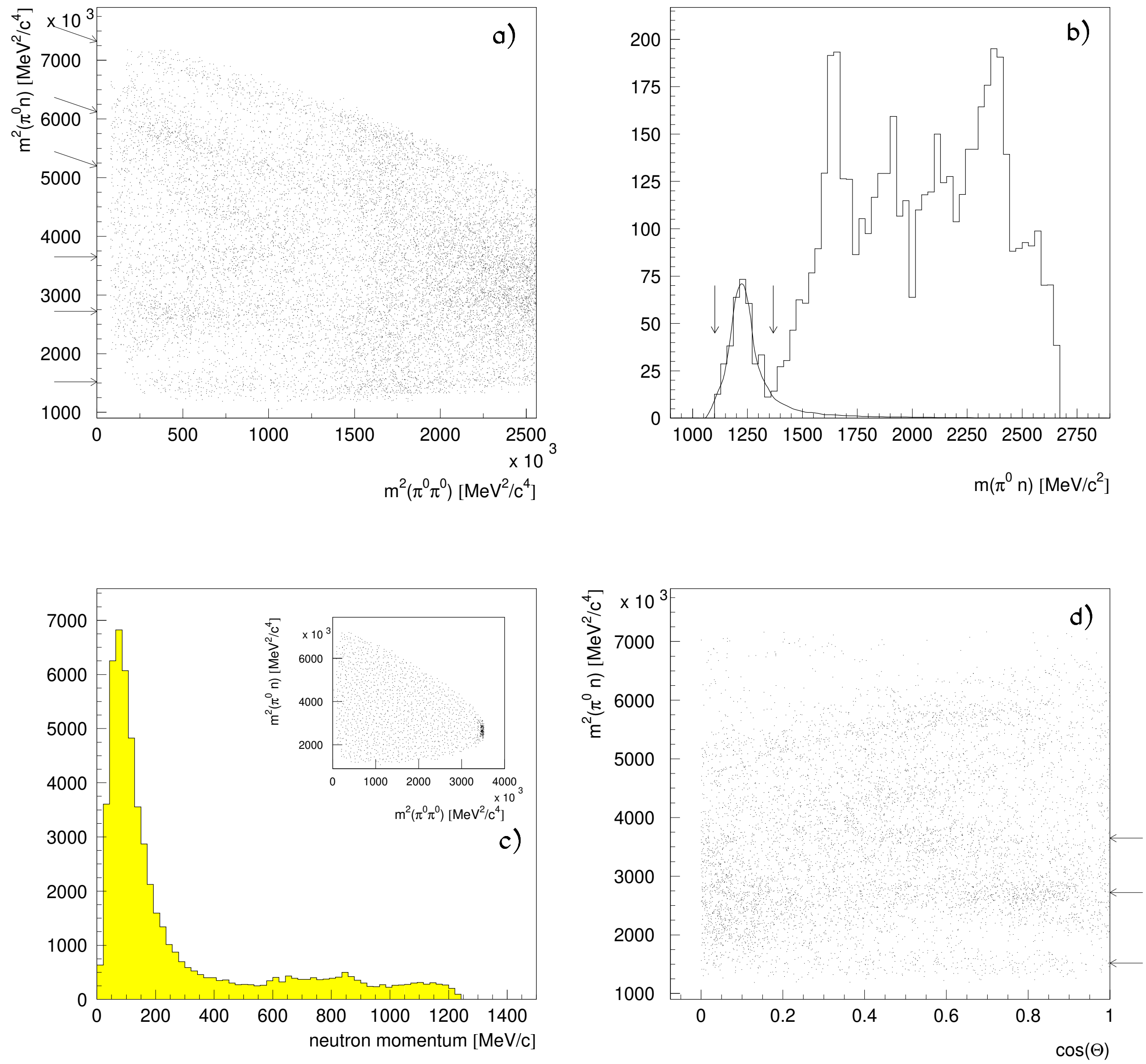

Fig. 3. a) $\pi^0\pi^0$n-Dalitzplot, with cut at $|\ \boldsymbol{p}_n\ | \geq 600$ MeV/c, b) invariant π^0n mass with $m_{\pi^0\pi^0} \leq 1000$ MeV/c^2, the superposed line represents the fit to the $\Delta(1232)$, the arrows indicate the limits of the mass range fitted, c) neutron momentum distribution, inset: complete $\pi^0\pi^0$n-Dalitzplot, d) invariant π^0n mass versus the cos(Θ). All plots are corrected for the momentum dependent neutron detection efficiency.

masses, widths and spin-parity of possible baryon resonances is not possible. Therefore, we restrict ourselves to a discussion of the $\Delta(1232)$.

The solid line in figure 3b represents a fit to the π^0n mass spectrum. The two arrows indicate the mass range of the fit. We find

$$m = 1230.6 \pm 4.1\text{MeV} \tag{4}$$

$$\Gamma = 120.8 \pm 12.8\text{MeV} \tag{5}$$

in good agreement with the accepted values for the $\Delta(1232)$ [4]. Monte-Carlo simulations of the reaction $\bar{\text{p}}\text{d}\rightarrow f_2(1270)$+n have shown that this contribution is negligible in the mass region used for the fit.

While the nucleon resonances are seen clearly at low $\pi^0\pi^0$ invariant masses, the background is large for high $\pi^0\pi^0$ invariant masses, i.e. for small neutron momenta. Low and high $\pi^0\pi^0$ masses correspond to different regions of the $\Delta(1232)\rightarrow$ nπ^0 decay angular distribution. Since the $\Delta(1232)\rightarrow$ nπ^0 decay is parity conserving, the angular distribution must be symmetric. Hence we can exclude the large–background region by rejecting events with $\cos(\Theta)\leq 0$.

In figure 3d we show the scatterplot where the squared $n\pi^0$ invariant mass is plotted against the cosine of the $\Delta(1232)\rightarrow$nπ^0 decay angle (Θ) in the Gottfried-Jackson frame. Only the range $0 \leq\cos(\Theta)\leq 1$ is shown corresponding to π^0 backward emission. The three relevant mass enhancements are indicated by arrows; the reflections are no longer straight lines and are therefore less visible. The $f_2(1270)$ leaks into the scatterplot at its lower left side.

We fit the mass projection of figure 3d with fixed mass and width for the $\Delta(1232)$ and find 636.4 ± 40.6 events, after integrating over the full $\Delta(1232)$ width. Hence 1272.8 ± 81.2 events would be observed in the full angular distribution.

The $\Delta(1232)\rightarrow$nπ^0 decay angular distribution is shown in fig. 4 after a cut at 1232 ± 120 MeV.

The distribution is nearly flat with a small contribution from $\bar{\text{p}}\text{d} \rightarrow f_2(1270)$n events at $\cos(\Theta)\approx 0$. From the angular distribution we estimate the backgound to contribute about ≈ 32 events. We have checked the angular distribution by cutting on $\cos(\Theta) \geq 0.1$; 0.2; 0.3; 0.4; 0.5; or 0.6. The re-

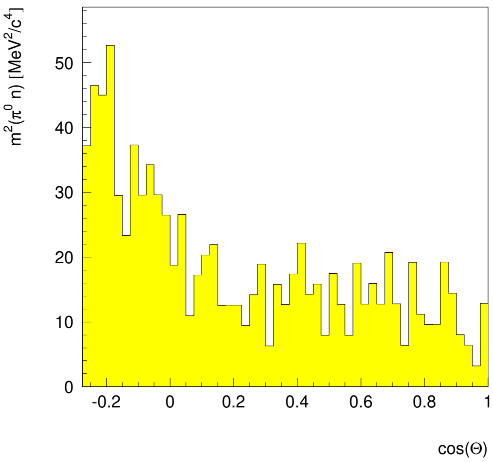

Fig. 4. *Decay angular distribution of $\Delta^0\rightarrow n\pi^0$. Note that foreward angles are not shown due to the large background from $\bar{p}d\rightarrow\pi^0\pi^0 n$ events in which the neutron is a spectator.*

sulting spectra were then fitted in order to determine the number of $\Delta(1232)$. Within statistics the number of events scales with the $\cos(\Theta)$ interval.

The flat angular distribution suggests that the $\Delta(1232)$ - a P_{33} nucleon resonance - is produced with no angular momentum with respect to the recoiling π^0. The most likely reaction chain is therefore

$$\bar{\text{p}}\text{d}(^{24}S_{3/2})\rightarrow \Delta\pi^0; \quad \Delta \rightarrow \pi^0\text{n} \ . \tag{6}$$

However, contributions from other $\bar{\text{p}}$d atomic states cannot be excluded.

We determine the effective number of $\bar{\text{p}}$d annihilations in the zero–prong data by comparing the number of $\pi^0\pi^0$n events in the zero–prong data and the minimum bias data. We multiply this ratio by the total number of $\bar{\text{p}}$d annihilations taken with the minimum bias trigger. This number is corrected by a factor of 0.956 ± 0.025 for antiprotons lost in beam counters or the target walls. Thus a final number of $(208.3 \pm 11.3)\cdot 10^6$ antiprotons stopping in liquid deuterium led to the observed number of events.

The branching ratios for reactions(1-3) are derived from the relation:

	N_{events}	ε_{MC}	BR_d
$\pi^0\pi^0$n	56966.3±254.3	0.48	0.988^2
$\pi^0\eta$n	8570.3 ±101.3	0.44	$0.988 \cdot 0.388$
$\pi^0\Delta^0$	1314.4±121.5	0.44	$2/3 \cdot 0.988^2$

Table 2
Observed events, efficiencies for reconstruction of the neutral mesons ε_{MC} and decay branching ratios for the different channels. The error of ε_{MC} is less than 0.3%. The factor 2/3 is square of the Clebsch Gordan coefficient for $\Delta^0 \to \pi^0$n. The number of events is corrected additionally for events where the neutron produces more than one energy deposit in the calorimeter, which has an effect on events with high neutron momenta.

$$BR = \frac{N_{\rm events}}{\varepsilon_{\rm MC} \cdot BR_{\rm d} \cdot N_{\rm an}} \ . \quad (7)$$

N_{events} is the number of events assigned to the reaction; ε_{MC} the efficiency to detect the 4 photons and to reconstruct the two mesons; BR_d is the product decay branching ratio of $\pi^0 \to \gamma\gamma$, $\eta \to \gamma\gamma$ and $\Delta \to \pi^0$n, respectively. With these numbers the final branching ratios are obtained as follows:

$$BR(\bar{\rm p}{\rm d} \to 2\pi^0 + {\rm n}) = (5.90 \pm 0.32) \cdot 10^{-4} \quad (8)$$

$$BR(\bar{\rm p}{\rm d} \to \pi^0\eta + {\rm n}) = (2.46 \pm 0.12) \cdot 10^{-4} \quad (9)$$

$$BR(\bar{\rm p}{\rm d} \to \Delta(1232)\pi^0) = (2.21 \pm 0.24) \cdot 10^{-5} \ . \quad (10)$$

None of these branching ratios has been reported before.
We may compare the branching ratio of reaction (10) with that of the Pontecorvo reaction $\bar{\rm p}{\rm d} \to {\rm n}\pi^0$ [3]. We find:

$$\frac{BR(\bar{\rm p}{\rm d} \to {\rm n}\pi^0)}{BR(\bar{\rm p}{\rm d} \to \Delta\pi^0)} = 0.32 \pm 0.05 \quad (11)$$

The preference for the production of $\Delta(1232)$ compared to neutron may be related to two observations: $\Delta(1232)$ production is allowed from the $^{24}S_{3/2}$ state with no angular momentum, n production with ℓ=0 proceeds only via $^{22}S_{1/2}$. Hence we naively expect a factor of two. Furthermore, the higher mass of the $\Delta(1232)$ may be favoured since the intermediate state is closer to the mass shell than for production of the nucleon. A similar trend has also been found in Pontecorvo production of mesons [3].

Acknowledgement

We would like to thank the technical staff of the LEAR machine group and of all the participating institutions for their invaluable contributions to the success of the experiment. We acknowledge financial support from the German Bundesministerium für Forschung und Technologie, the Schweizerischer Nationalfonds, the British Particle Physics and Astronomy Research Council and the U.S. Department of Energy (contract No. DE-FG03-87ER40323, DE-AC03-76SF00098, and DE-FG02-87ER40315). F.-H. Heinsius and K.M. Crowe acknowledge support from the A. von Humboldt Foundation.

References

[1] J. Riedelberger et al., Phys. Rev. **C40** (1989)
[2] E. Aker et al. (Crystal Barrel Collaboration), Nucl. Instrum. Methods **A321**(1992)69
[3] C. Amsler et al. (Crystal Barrel Collaboration), accepted for publication in Zeit. Phys. A
[4] Review of Particle Properties: L. Montanet et al. Phys. Rev. **D50** (1994)1198